Fatigue crack nucleation and growth in filled natural rubber

W. V. MARS[1] and A. FATEMI[2]

[1]Cooper Tire and Rubber Company, Finland, OH, USA, [2]The University of Toledo, Toledo, OH, USA

Received in final form 31 January 2003

ABSTRACT Rubber components subjected to fluctuating loads often fail due to nucleation and the growth of defects or cracks. The prevention of such failures depends upon an understanding of the mechanics underlying the failure process. This investigation explores the nucleation and growth of cracks in filled natural rubber. Both fatigue macro-crack nucleation as well as fatigue crack growth experiments were conducted using simple tension and planar tension specimens, respectively. Crack nucleation as well as crack growth life prediction analysis approaches were used to correlate the experimental data. Several aspects of the fatigue process, such as failure mode and the effects of R ratio (minimum strain) on fatigue life, are also discussed. It is shown that a small positive R ratio can have a significant beneficial effect on fatigue life and crack growth rate, particularly at low strain range.

Keywords rubber crack growth; rubber crack nucleation; rubber fatigue life.

NOMENCLATURE

a_0 = initial flaw size
b = planar tension specimen height
L = simple tension specimen instantaneous length
L_0 = simple tension specimen effective undeformed grip-to-grip length
L_{eff} = simple tension specimen effective undeformed gauge section length
L_{alt}, L_{mean} = alternating, mean length of simple tension specimen
L_{min}, L_{max} = minimum, maximum length of simple tension specimen
m = number of fatigue tests
N_{f} = life to fracture
$N_{\text{f,max}}$, $N_{\text{f,min}}$ = maximum, minimum fatigue life
N = median fatigue life
r_{c} = maximum fatigue crack growth rate
R = ratio of minimum to maximum
R_ε, R_δ, R_{W} = R-ratio based on strain, displacement, strain energy density
T = energy release rate
W = strain energy density
ε = gauge section strain
ε_{c} = strain at fracture
ε_{min}, ε_{max} = minimum, maximum gauge section strain
δ = gauge section displacement

INTRODUCTION

The ability of rubber to withstand very large strains without permanent deformation makes it ideal for many applications such as tires, vibration isolators, seals, hoses and belts. As these applications impose large static and time-varying strains, durability and therefore mechanical fatigue is often the primary consideration. Software-based simulation tools for predicting mechanical fatigue life of rubber components are not presently available, despite the fact that fatigue testing may be the most expensive of all product testing. Such tools have been developed

Correspondence: A. Fatemi. E-mail: afatemi@eng.utoledo.edu

for other materials, metals in particular. However, these are commonly based upon theories of material behaviour that cannot be applied to rubber, due to rubber's highly deformable and nonlinear nature.

Typically, the fatigue failure process involves a period during which cracks nucleate in regions that were initially free of observed cracks, followed by a period during which nucleated cracks grow to the point of failure. Analysis approaches that are currently available for predicting fatigue life in rubber, including both crack nucleation as well as crack growth approaches, are reviewed in Ref. [1]. In a crack nucleation approach, mechanical severity is defined in terms of some quantity, such as stress or strain, that is known at a material point, in the sense of continuum mechanics. Failure is taken as the number of cycles required for cracks of a given size to appear, for the stiffness of the specimen to decrease by a specified amount, or for specimen rupture to occur. In rubber, uniaxial fatigue life results are commonly correlated based on maximum principal strain (or stretch) and strain energy density. Strain is a natural choice because it can be directly determined from displacements, which can be readily measured in rubber. When strain energy density is applied in fatigue analysis in rubber, it is often estimated from a hyperelastic strain energy density function, which is defined entirely in terms of strains. Stress, apparently, has rarely been used as a fatigue life parameter in rubber. This may be due partly to traditionally testing rubber in displacement control, and to the difficulty of accurate stress determination in rubber components.

In a fracture mechanics approach, mechanical severity is defined in terms of the loading and geometry of a pre-existing crack or flaw. The idea of focusing attention on individual flaws was introduced by Inglis[2] in 1913, and Griffith[3] in 1920. Griffith's fracture criterion is based on an energy balance including both the mechanical energy of a cracked body and the energy associated with the crack surfaces and was extended to rubber by Thomas, Greensmith, Lake, Lindley, Mullins, Gent and Rivlin in the 1950s and 1960s.[4–16] While, the original application of this approach was to predict static strength, Thomas[8] extended the approach to analyse the growth of cracks under cyclic loads in natural rubber. He discovered a square-law relationship between peak energy release rate and crack growth rate for natural rubber. This predated Paris' power-law relationship between the stress intensity factor range and crack growth rate in metals[17] by 3 years. Both the energy release rate, which is most commonly used in rubber fracture analyses, and the stress intensity factor commonly used for metals, relate the global structural loading to the local crack tip strain and stress fields. While the stress intensity factor is only applicable in situations of linear elasticity, the energy release rate is applicable for nonlinear elastic materials and finite strains.

Many factors influence the fatigue behaviour of rubber. A review of these factors is given in Ref. [18]. They include various aspects of the mechanical loading history, environmental effects, effects of rubber formulation and effects due to the dissipative aspects of the constitutive response of rubber. A primary consideration relating to the mechanical load history is rubber's extreme sensitivity to not only the load range, but also the R ratio. Depending on the polymer type and the presence of fillers, the effect of increasing the minimum or mean loading may be either beneficial or harmful. Other aspects of the mechanical load history include the effects of static loaded periods (annealing), load sequence, multiaxiality, frequency and loading waveform. Environmental factors can affect both the short- and long-term fatigue behaviour of rubber. In the short term, elevated temperatures and the presence of oxygen or ozone are detrimental. The rate of crack growth may vary reversibly with these variables, in the short term. At long life, irreversible changes to the elastomer due to elevated temperature and oxidative ageing become important considerations. These changes include evolution of both the elastic and fatigue properties. Rubber is unique in that a great range of behaviour is available by proper manipulation of formulation and processing variables. Proper selection of elastomer type, filler type and volume fraction, antidegradants, curatives and vulcanization can ensure maximum fatigue life. The role of dissipative constitutive behaviour and distinct dissipative mechanisms is critical to the understanding and improvement of fatigue behaviour of rubber. These mechanisms include initial transient softening (the Mullins effect), strain crystallization, rate-independent hysteresis and viscoelasticity. These aspects are discussed in detail in Ref. [18].

Experimental methods for characterizing the mechanical fatigue behaviour of rubber correspond closely to the aforementioned nucleation and propagation analysis approaches. In both approaches, uniaxial, constant-amplitude, pulsating tension experiments on simple test specimens provide a baseline against which the results of more complicated experiments can be compared. This paper presents the results of fatigue experiments on a filled, natural rubber compound, following both approaches. Macro-crack nucleation experiments were conducted at several levels of minimum strain (R ratio). These experiments demonstrated the important effect of minimum strain on fatigue life. Based on observations of the failure mode, the dependence of fatigue life on the presence of cracks in the virgin material is discussed. Crack growth experiments were also conducted to characterize the dependence of crack growth rate on the history of loading and R ratio.

It should be noted that the term 'macro-crack nucleation' in this work is defined as crack(s) on the order of 1 mm or longer. In contrast, pre-existing defects or micro-cracks in

the material are on the order of 0.1 mm or smaller. Therefore, from a physical standpoint, fatigue crack nucleation life here can be interpreted as the growth period of these pre-existing micro-cracks (smaller than 0.1 mm in size). The distinction between 'crack nucleation' versus 'crack growth' approaches is based on the practical application of the two approaches. In a crack nucleation approach, the analysis is without regard to features such as initial crack or defect size, shape, orientation or distribution. In a crack growth approach, however, such features of the crack or defect are essential inputs to the analysis.

EXPERIMENTAL PROGRAM

ASTM D4482 standard[19] rubber fatigue specimens, as shown in Fig. 1, were used in this investigation for macro-crack nucleation experiments. The stress state in the gauge length of this specimen is one of simple tension. Testing was performed on a mechanically driven, custom-designed test machine. The machine applied a displacement-controlled, sinusoidal waveform. The machine simultaneously tested specimens at three distinct levels of alternating displacement. The minimum displacement was manually adjustable at each rack of specimens. There were six racks of specimens. Tests were run at laboratory temperature, nominally 20 °C. The test frequency was 1.7 Hz. Ten specimens were run at each displacement level. Tests were conducted at two nominal R ratios, $R_\varepsilon = 0$ and $R_\varepsilon = 0.07$. Note that only $R \geq 0$ tests are possible with the ASTM specimen, because the specimen will not support a compressive load. In these experiments, failure was defined as the number of cycles to complete fracture of the specimen. Failure was detected via a switch that stops a counter when the specimen is completely broken. Details of the tests conducted, and the results obtained, can be found in Table 1.

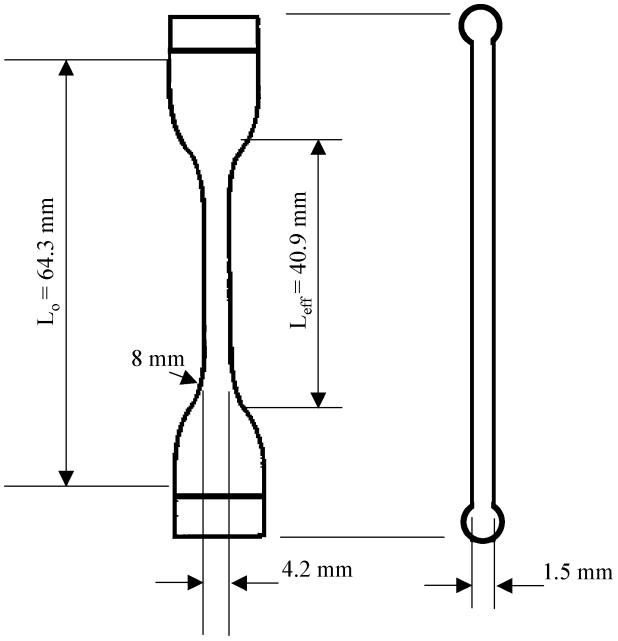

Fig. 1 ASTM D4482 simple tension fatigue specimen geometry.

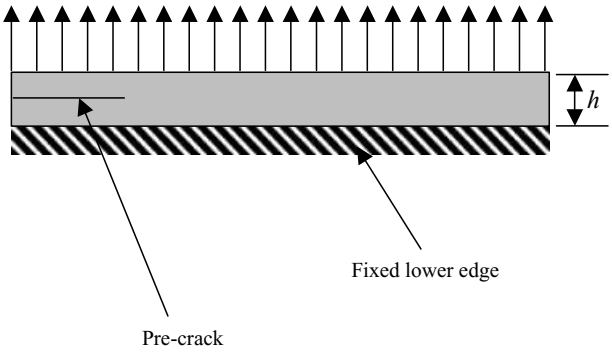

Fig. 2 Planar tension test specimen geometry with pre-crack.

While no test standard yet exists for measuring the fatigue crack growth curve in rubber, the procedures and analysis methods are reasonably well documented in the literature, and are in widespread use, at least for the case of $R = 0$ cyclic loading. A planar tension test specimen, in which the load is applied along an axis normal to the long edge, and in which the clamps prevent displacement in the direction of the long edge, was used for crack growth experiments in this study (Fig. 2). The nominal specimen dimensions were 150 × 10 × 1 mm. Testing was run on a uniaxial, servohydraulic test machine with a nominal laboratory air temperature of 20 °C. The applied waveform was constant amplitude, 10 Hz haversine pulse. Tests were run in displacement control, at minimum strain levels of 0.00 and 0.03. In each test, the maximum strain was varied in steps of increasing magnitude, the maximum strain remaining constant within each step. Because the minimum strain was held constant in these tests, and the maximum strain steps varied from zero to failure, the R-ratio is not constant in these tests, except for the zero minimum strain condition, for which $R = 0$. It should be noted that even though the R-ratio here is defined based on engineering strain, R_ε, another measure of R-ratio, which is perhaps more meaningful at finite strain, could be defined in terms of strain energy release rate, R_W. Values of R_W for the tests conducted are also included in Table 1.

An initial crack was produced in the planar tension test specimen by cutting the specimen along the mid-plane, with a surgical scalpel. The initial crack was introduced at one edge to a depth of approximately 25 mm, to avoid specimen end effects. Experimental strain measurements were obtained via a non-contact laser extensometer. Displacement measurements were obtained directly from test frame LVDT readings. Crack growth was automatically recorded at varying intervals via a video camera and

Table 1 Uniaxial fatigue crack nucleation life under nominal $R = 0$ and $R > 0$ conditions

Position	1A	2A	3A	1B	2B	3B
			$R = 0$			
L_{min}	2.70	2.60	2.53	2.47	2.60	2.47
L_{max}	6.24	4.91	3.47	6.20	4.66	3.41
L_{alt}	1.77	1.15	0.47	1.87	1.03	0.47
L_{mean}	4.47	3.75	3.00	4.33	3.63	2.94
ε_{min}	0.10	0.04	0.00	−0.04	0.04	−0.04
ε_{max}	2.30	1.47	0.58	2.28	1.32	0.54
R_ε	0.05	0.03	0.00	0.00	0.03	0.00
R_W	0.01	0.00	0.00	0.00	0.01	0.00
Test			N_f			
1	1109	7145	62345	1177	5288	95757
2	1118	7161	67845	1252	5709	113059
3	1118	7272	73219	1575	6489	128469
4	1121	7586	74681	1587	6783	143886
5	1233	8463	78680	1643	7300	164478
6	1435	9859	78702	1725	8609	172802
7	1815	10454	82139	1727	9803	175386
8	2099	10495	92264	1727	9888	200517
9	2234	10948	93246	1727	10208	200518
10	2353	11238	95634	1873	10687	215449
Median	1334	9161	78691	1684	7955	168640
Geometric mean	1493	8917	79174	1586	7845	156192
$N_{f,max}/N_{f,min}$	2.1	1.6	1.5	1.6	2.0	2.2
			$R > 0$			
L_{min}	3.10	2.72	2.40	3.01	2.66	2.61
L_{max}	6.50	4.85	3.31	6.35	4.94	3.60
L_{alt}	1.70	1.07	0.46	1.67	1.14	0.50
L_{mean}	4.80	3.79	2.86	4.68	3.80	3.11
ε_{min}	0.35	0.12	−0.08	0.30	0.08	0.05
ε_{max}	2.46	1.44	0.48	2.37	1.49	0.66
R_ε	0.14	0.08	0.00	0.13	0.05	0.07
R_W	0.05	0.02	0.00	0.04	0.01	0.02
Test			N_f			
1	1385	27822	48388	1126	12267	668163
2	1820	29828	68314	1126	14025	682833
3	2144	50550	96848	1156	14671	737061
4	2220	50998	101581	2932	15177	739902
5	2671	52815	116695	3093	16516	757663
6	2865	54543	121213	3843	16518	782385
7	3185	54863	125009	4142	16891	815146
8	4418	55217	129857	4721	17208	872671
9	4422	55854	134749	5302	18511	948692
10	4648	57529	138818	7599	30577	1191547
Median	2865	54543	121213	3843	16518	782385
Geometric mean	2769	47622	103398	2887	16731	807996
$N_{f,max}/N_{f,min}$	3.4	2.1	2.9	6.7	2.5	1.8

image analysis system. The camera was equipped with optics such that the field of view covered approximately 12 × 16 mm of the specimen surface. Camera images contained 480 pixels in the crack growth direction, giving a theoretical resolution of 0.025 mm on the change in crack length that could be detected. An advantage of the planar tension specimen, relative to other fracture mechanics test specimens for rubber is that, under displacement control,

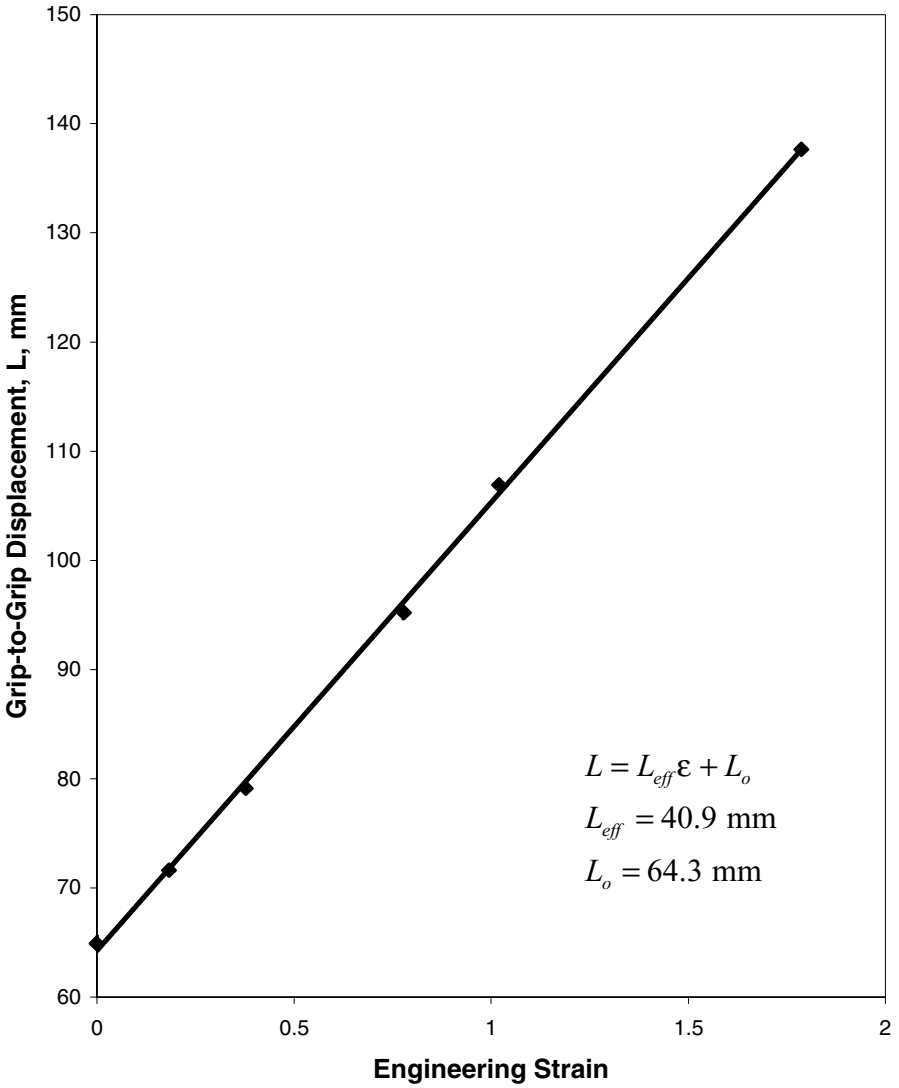

Fig. 3 Determination of the strain–displacement relationship for a simple tension specimen used in crack nucleation experiments.

the energy release rate is independent of crack size. This is true for linear elastic material behaviour, as well as non-linear elastic behaviour of rubber, due to the fact that the effect of crack growth is merely to translate the crack tip fields in this specimen. As the energy release rate is independent of crack size, the fatigue crack growth rate is also constant, on average, and the crack length varies linearly with applied cycles.[8,20,21] Crack growth at a constant rate may therefore be observed until a statistically converged measurement of the crack growth rate is obtained.

ANALYSIS AND DISCUSSION OF EXPERIMENTAL RESULTS

Macro-crack nucleation experiments

In order to determine the gauge section strain ε from knowledge of the instantaneous specimen length L, an empirical strain-displacement relationship was developed, of the form given below

$$\varepsilon = \frac{L - L_0}{L_{\text{eff}}}, \tag{1}$$

where L_0 is the effective undeformed grip-to-grip distance, and L_{eff} is the effective undeformed gauge length. The constants L_0 and L_{eff} were computed via linear regression from experimentally determined values of L and ε. Strain ε was directly measured via the visual technique of measuring the distance between two gauge marks on the specimen. These data and the corresponding best-fit line are plotted in Fig. 3. The best-fit constants are $L_0 = 64.3$ mm and $L_{\text{eff}} = 40.9$ mm. In Fig. 1, it can be seen that these constants compare reasonably well with the physical dimensions of the specimen.

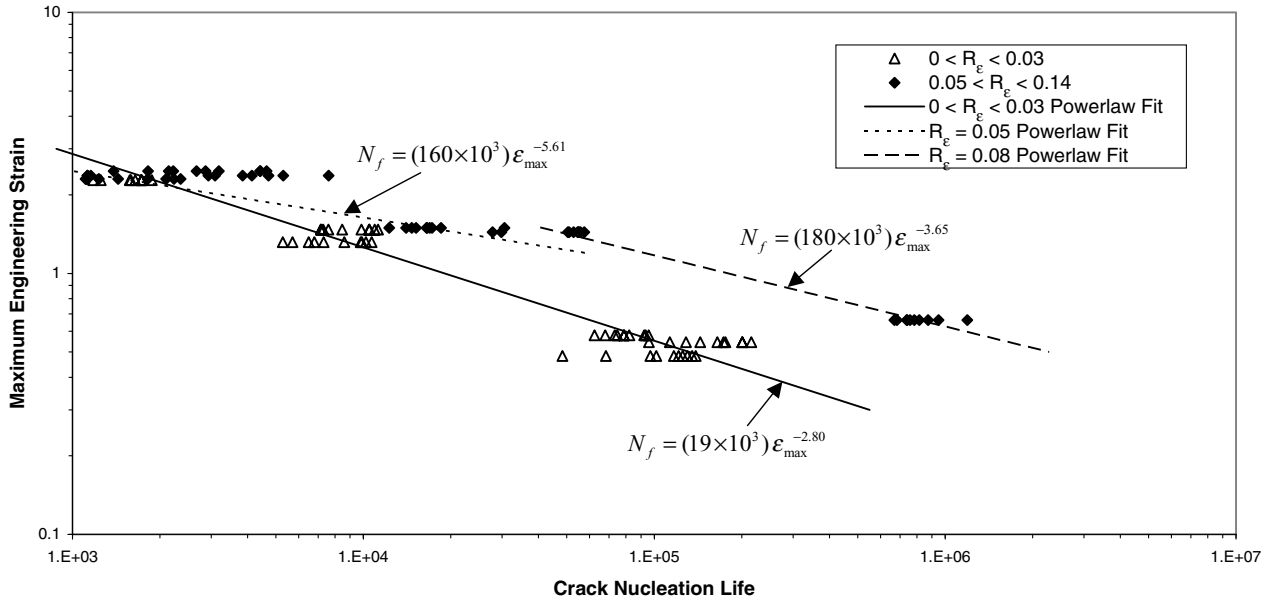

Fig. 4 Effect of peak strain on simple tension crack nucleation life. Individual results.

As recommended in the ASTM D4482 standard, the geometric mean of the observed fatigue lives is reported in Table 1. Note that the geometric mean is associated with the mode of the log-normal distribution. The median is also reported in this table. The geometric mean is defined as

$$\bar{N} = \log^{-1}\left(\frac{\sum_{i=1}^{m}\log N_i}{m}\right). \tag{2}$$

The R-ratio was defined in terms of gauge section strain as $R_\varepsilon = \varepsilon_{min}/\varepsilon_{max}$. It will be seen that the seemingly small difference in R values of 0 and 0.07 used in this study gives rise to significant differences in fatigue life. Because of the lower limit on R, the $R_\varepsilon = 0$ condition could be readily achieved by setting the minimum machine displacement slightly shorter than the undeformed specimen length. The $R_\varepsilon = 0.07$ condition, however, was more difficult to achieve with the available experimental arrangement. Actual values of R_ε are tabulated with the experimental data in Table 1.

The ratio $N_{f,max}/N_{f,min}$ is also tabulated in Table 1, and provides a measure of the observed scatter. This ratio typically fell in the range $1.5 < N_{f,max}/N_{f,min} < 3.4$, though a case for which $N_{f,max}/N_{f,min} = 6.7$ was also observed. To the extent that the fatigue life reflects the size of flaws present in the virgin material, the scatter may reflect variation in the size of actual initial flaws. As natural rubber has one of the lowest fatigue crack growth rate exponents relative to other types of rubber, it is expected that the scatter in fatigue life at a given operating condition would be lower for natural rubber than for other types of rubber.

Macro-crack nucleation life is plotted as a function of peak strain in Fig. 4, which shows individual test results and in Fig. 5, which shows averaged results. Both plots also show the best-fit power-law lines for three levels of R-ratio, using a least squares fit with fatigue life as the dependent variable. Plots of averaged data as a function of peak strain energy density and as a function of peak stress look very similar to that for peak strain in Fig. 5. It can be seen that the effect of $R > 0$ cycles is to increase the life. The life improvement is very significant at low strain, about an order of magnitude, and is less important at high strain, about a factor of two. This behaviour is opposite to that observed for metals, where a positive R-ratio (i.e., tensile mean stress) generally decreases fatigue life. The observed results are consistent with results reported elsewhere,[22,23] that for strain-crystallizing rubbers, $R > 0$ cycles greatly enhance the fatigue life. Note, because $R_\varepsilon \approx 0$ in this work, the peak or maximum and the range of the values of strain, stress or strain energy density are nearly the same.

Care is required in making a physical interpretation of stress and strain at finite strains. However, as long as one is consistent and the measures are energetically conjugate, then the choice of strain or stress is largely a matter of convenience. For example, integrating Cauchy stress with Hencky strain, or Engineering strain with Engineering stress to obtain strain energy density would give identical results. Here Engineering quantities were chosen because they could be directly computed from measured displacements and loads. In addition, engineering measures are often considered to be more intuitive.

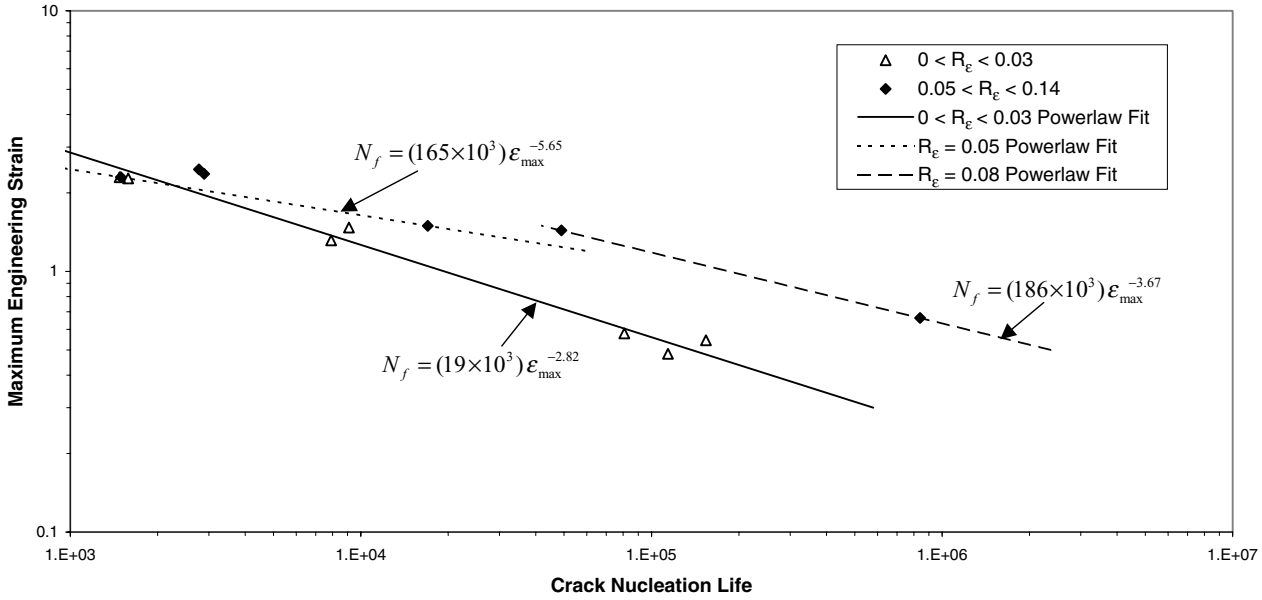

Fig. 5 Effect of peak strain on simple tension crack nucleation life. Averaged results.

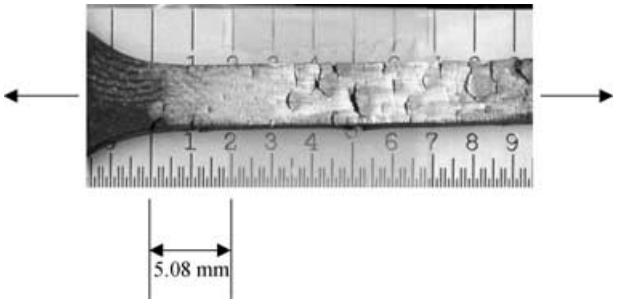

Fig. 6 Surface cracking in a failed simple tension fatigue specimen.

In macro-crack nucleation experiments, the failure mode is the propagation of flaws presumably present in microscopic form in the virgin material. Such flaws are thought to be distributed throughout the material, and on the surfaces of the specimen. Prior to specimen failure, it is hypothesized that cracks propagate from these initial flaws at varying rates, depending upon the particular size, shape and orientation of each flaw. Fatigue life, by the present definition, is determined ultimately by the first crack to grow sufficiently large to cause specimen fracture. Interactions between the initial micro-flaws and their effect on fatigue life were not considered; as mentioned earlier, features of the initial flaws or cracks (i.e., size, shape, orientation and distribution) are not explicitly used or required for macro-crack nucleation approaches.

While the first crack to traverse the specimen cross-section determines the fatigue life, many cracks are visible on the failed specimen surface, as shown in Fig. 6. The pictured specimen is completely failed, and is shown as slightly strained to permit observation of the cracks. It can be seen that the cracks are primarily oriented perpendicular to the applied load, that they initiate both on specimen surfaces and on edges, and that the length of many cracks comprises a significant fraction (>25%) of the specimen width. The fact that cracks initiate both on the specimen surfaces and on the edges is evidence that the initial flaws are indeed intrinsic to the material, and that they were not introduced from the specimen die-cutting process. The large size and number of observed surface cracks suggest that the flaw from which the largest crack grew was not initially much larger than the initial flaws from which other visible surface cracks grew. The surface cracks are therefore somewhat indicative of the initial distribution of crack sizes, and their spatial density. Because ultimate specimen failure is determined by fracture, the question of flaw density may be of secondary importance, in that the flaw density is not needed to predict the evolution of a single critical flaw. Of course, such a model ignores crack interaction considerations such as the possibility that the final fracture may have multiple initiation sites.

Crack growth experiments

The energy release rate T of the planar tension specimen was computed from the traditional expression

$$T = Wh, \tag{3}$$

where h is the specimen height (Fig. 2). Specimen strain energy density W was computed via integration of the loading path of the engineering stress–strain curve. The stress–strain curve was computed from displacement and

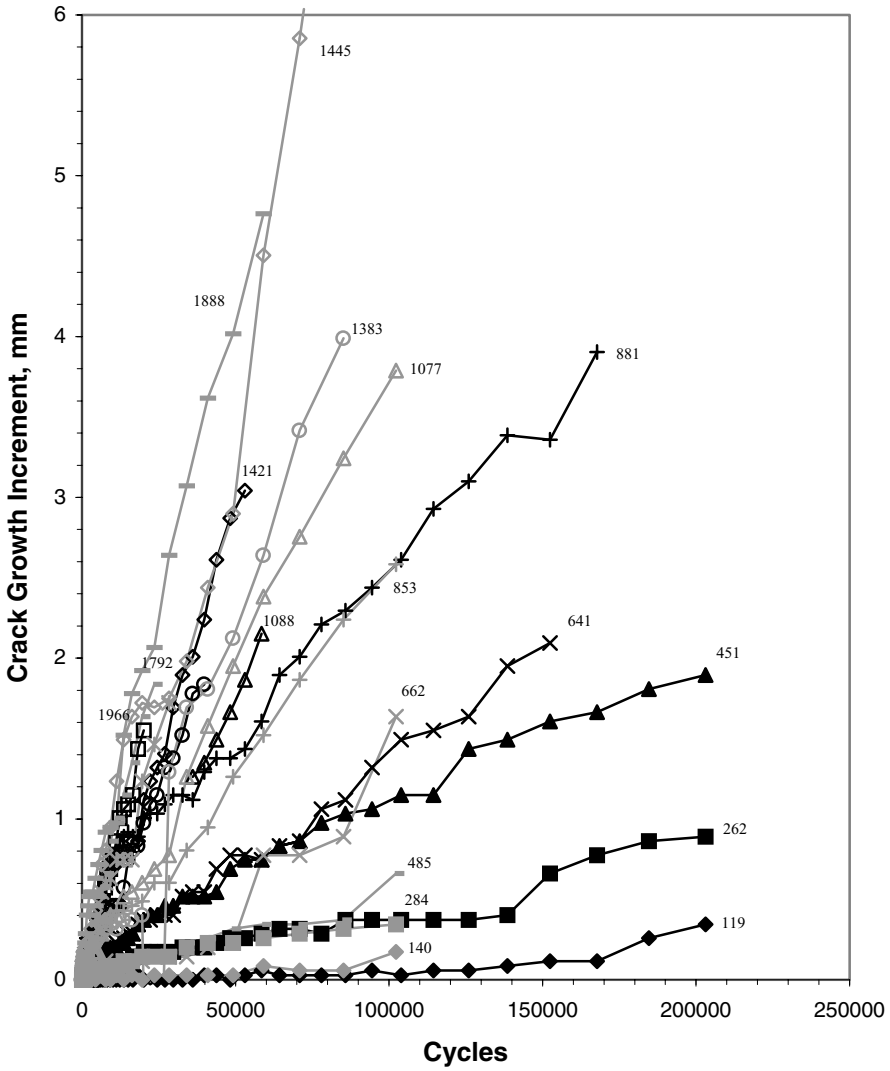

Fig. 7 Typical crack growth histories for $\varepsilon_{min} = 0.00$. Labels give the corresponding energy release rate range, J m^{-2}.

force measurements made in situ on the cracked specimen, taken immediately before the measurement of the crack length. The undeformed cross-sectional area for the stress calculation was computed based on the measured specimen thickness, and the difference between the initial specimen width and the instantaneous crack length. As mentioned earlier, the crack growth rate at a constant energy release rate was determined from the slope of a linear regression of crack size, plotted against applied cycles. Plots of crack length versus applied cycles for $R = 0$ tests at different ε_{max} levels are shown in Fig. 7.

Figure 8 shows the observed fatigue crack growth rate as a function of the applied energy release rate range. Results for two displacement-controlled levels of ε_{min} (0.00, 0.03) are shown. Tests at $\varepsilon_{min} = 0.06$ were also run, but negligible crack growth occurred during the test period, even at the highest levels of applied strain range. It is again observed that the effect of $R > 0$ cycles is to decrease the fatigue crack growth rate. The improvement is very significant at low strain range, as much as an order of magnitude for $\varepsilon_{min} = 0.03$. The improvement was even greater for $\varepsilon_{min} = 0.06$. The improvement becomes less significant at large energy release rate range, consistent with the fact that, at constant ε_{min}, the R-ratio decreases as the energy release rate range increases. A new phenomenological model for describing $R > 0$ fatigue crack growth rate behaviour is developed in.[24] This model captures the well-established and significant beneficial effect of $R > 0$ loading on strain-crystallizing rubbers, and is shown to compare favourably with data from the literature and with the results of fatigue crack growth rate experiments in this study. This is discussed in more detail in Refs [23, 24]. Crystallization occurs anew with each application of the load, then 'melts' with each load removal. In this sense, the crystallization is reversible.

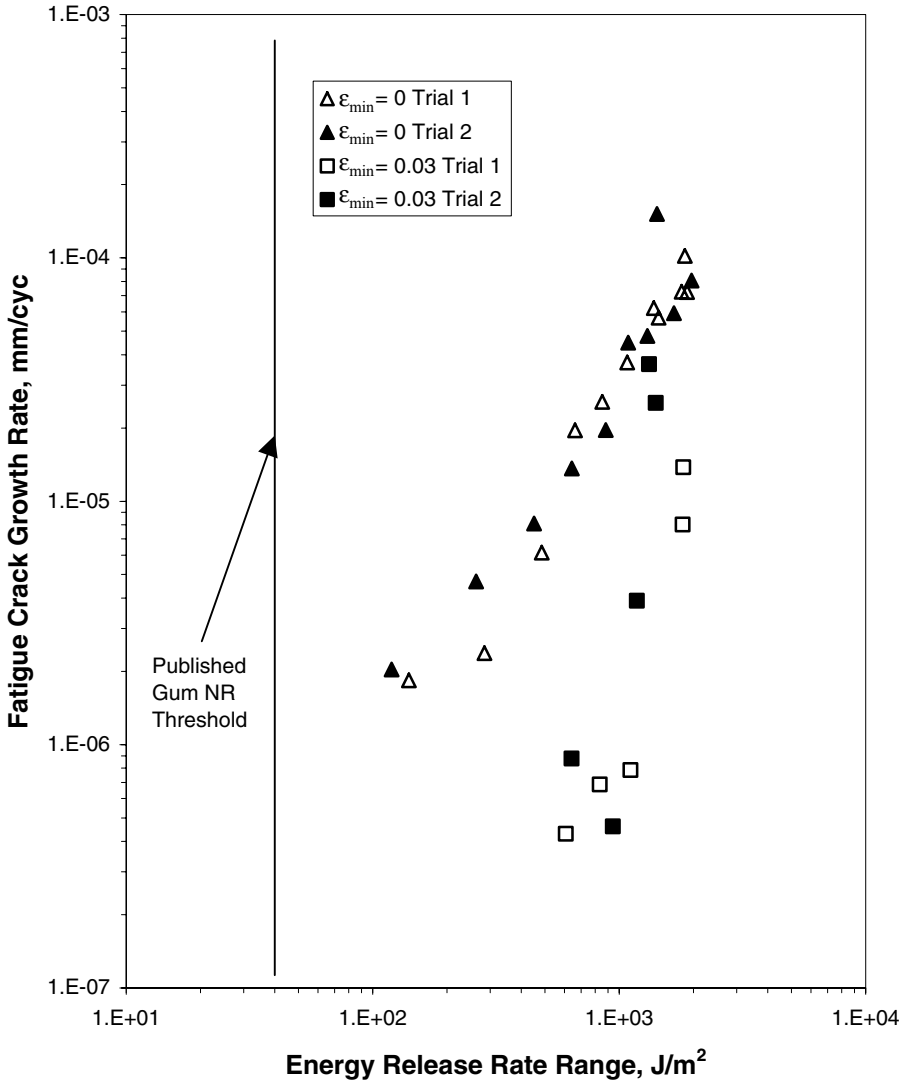

Fig. 8 Effect of ε_{min} on fatigue crack growth rate, at two levels of minimum strain.

No fatigue threshold was observed in this testing. For reference, the mechanical threshold that was found by Lake and Lindley[25] for gum natural rubber is plotted in Fig. 8. Apparently, measurement of the threshold for this material requires a longer observation period than the 8 h (or about 3×10^5 cycles) used in this study.

Comparison of crack nucleation and crack growth results

Crack nucleation life under uniaxial conditions can be predicted by integrating the fatigue crack growth relationship, assuming that the effective initial flaw size can be identified. From the relationship between crack nucleation life and the power-law fatigue crack growth properties derived in Ref. [1], an equation for N_f based on crack growth rate properties can be obtained[24] from the integration of a Paris-law expression for da/dN as follows:

$$N_f = \frac{a_0}{r_c} \frac{1}{F(R) - 1} \left(\frac{k(\varepsilon)W}{k(\varepsilon_c)W_c} \right)^{-F(R)}, \quad (4)$$

where a_0 is the initial flaw size, r_c is a maximum fatigue crack growth rate, $F(R)$ is an exponential function of R representing the R-ratio effect, k is a slowly varying, non-dimensional function of strain ε (see Ref. [1] for additional definition), and ε_c is the ultimate strain at fracture. In Fig. 9, where peak strain energy density is plotted versus crack nucleation life, predictions from this equation (shown with a dashed line) are compared with the experimentally obtained data from crack nucleation experiments (shown as solid line). Data from $R > 0$ crack nucleation tests have been plotted in terms of the equivalent $R = 0$ loading, as defined by the model proposed in Ref. [24].

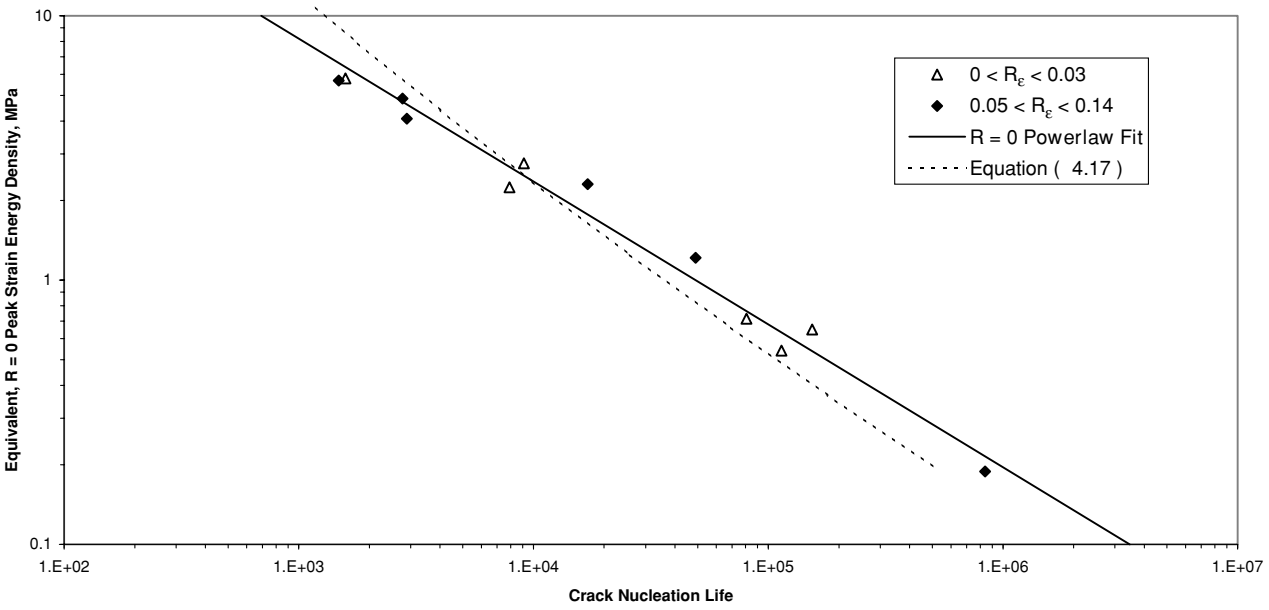

Fig. 9 Predicted and experimental fatigue life curves.

The inferred effective initial flaw size was used as the single curve-fit parameter to obtain agreement between the $R = 0$ crack nucleation and crack growth data. The resulting initial flaw size is 0.01 mm. This size is of the same order of magnitude as flaw sizes published by Lake and Lindley,[25] in the range 0.02–0.05 mm. This analysis assumes that in filled natural rubber, small cracks grow in a manner similar to long cracks, and is consistent with experimental observations in the literature.[26] Therefore, using a single curve-fit parameter (i.e., the initial flaw size), good agreement was obtained between nucleation life properties and fatigue crack growth properties.

The crack growth approach can be used as a total life approach, where the total fatigue life consists of the growth of pre-existing flaws to fracture. It can also be used as a complementary approach to the macro-crack nucleation approach, where the macro-crack growth life is evaluated and then added to the macro-crack nucleation life, to obtain the total life. The latter is often referred to as the 'two-stage' approach to fatigue life prediction.[27]

Comparing macro-crack nucleation and crack growth testing approaches, it should be pointed out that crack growth testing has certain advantages over macro-crack nucleation testing, at least from the standpoint of efficiency of material characterization. In crack growth approaches, the entire range of fatigue behaviour can be characterized using a small number of specimens. In crack nucleation approaches, many individual tests are required to construct the fatigue life curve. Also, a major source of variability in macro-crack nucleation tests is strong dependence on the initial size of uncontrolled flaws. Unintentional, uncontrolled flaws are easily introduced at any stage of the specimen manufacturing process (mixing, curing, cutting and storage), and may differ from those present in more complex parts produced using a different manufacturing process. Crack growth testing avoids this source of variability because the size of the crack is directly measured, and because the controlled, observed crack size is generally much larger than naturally occurring, unintentional flaws.

SUMMARY AND CONCLUSIONS

A number of aspects related to the fatigue failure process in rubber have been investigated in this work, using both the simple tension specimen for crack nucleation, as well as the planar tension specimen for crack growth. Based on the experimental data obtained and analyses performed, the following conclusions can be stated:

1 Experimental macro-crack nucleation lives in $R_\varepsilon \approx 0$ tests were correlated by using the applied peak (or range of) strain. Similar correlations were obtained by using peak (or range of) stress or strain energy density.
2 Experimental results demonstrated the important effect of minimum strain on fatigue life. Macro-crack nucleation tests with $R > 0$ cycles resulted in an increase in the fatigue life, as compared with $R = 0$ tests. The life improvement was very significant at low strain, about an order of magnitude, but less significant at high strain, about a factor of two.
3 Satisfactory correlation of the fatigue crack growth rates was obtained by using the range of the applied energy release rate as the correlating parameter.

4 The effect of $R > 0$ cycles in crack growth tests was to decrease the fatigue crack growth rates. This decrease was very significant at low strain range (more than an order of magnitude) and less significant at large energy release rate range.

5 Using an effective initial flaw size, good agreement was obtained between nucleation life properties obtained from simple tension specimens, and fatigue crack growth properties obtained from planar tension specimens.

6 Precursors to fatigue failure in rubber are unintentional flaws that exist in the virgin material. These flaws are a major source of fatigue life variability in macro-crack nucleation tests. Crack growth testing avoids this source of variability as the controlled/observed crack size is generally much larger than naturally occurring unintentional flaws.

REFERENCES

1 Mars, W. V. and Fatemi, A. (2002) A literature survey of fatigue analysis approaches for rubber. *Int. J. Fatigue* **24**, 949–961.

2 Inglis, C. E. (1913) Stresses in a plate due to the presence of cracks and sharp corners. *Trans. Inst. Nav. Archit.* **55**, 219–241.

3 Griffith, A. A. (1920) The phenomena of rupture and flow in solids. *Phil. Trans. R. Soc.* **221**, 163–198.

4 Rivlin, R. S. and Thomas, A. G. (1953) Rupture of rubber. I. Characteristic energy for tearing. *J. Polym. Sci.* **10**, 291–318.

5 Thomas, A. G. (1955) Rupture of rubber. II. The strain concentration at an inclusion. *J. Polym. Sci.* **18**, 177–188.

6 Greensmith, H. W. and Thomas, A. G. (1955) Rupture of rubber. III. Determination of tear properties. *J. Polym. Sci.* **18**, 189–200.

7 Greensmith, H. W. (1956) Rupture of rubber. IV. Tear properties of vulcanizates containing carbon black. *J. Polym. Sci.* **21**, 175–187.

8 Thomas, A. G. (1958) Rupture of rubber. V. Cut growth in natural rubber vulcanizates. *J. Polym. Sci.* **31**, 467–480.

9 Thomas, A. G. (1960) Rupture of rubber. VI. Further experiments on the tear criterion. *J. Polym. Sci.* **3**, 168–174.

10 Greensmith, H. W. (1960) Rupture of rubber. VII. Effect of rate of extension in tensile tests. *J. Polym. Sci.* **3**, 175–182.

11 Greensmith, H. W. (1960) Rupture of rubber. VIII. Comparisons of tear and tensile rupture measurements. *J. Polym. Sci.* **3**, 183–193.

12 Mullins, L. (1959) Rupture of rubber. IX. Role of hysteresis in the tearing of rubber. *Trans. Inst. Rubber Ind.* **35**, 213–222.

13 Greensmith, H. W. (1963) Rupture of rubber. X. The change in stored energy on making a small cut in a test piece held in simple extension. *J. Polym. Sci.* **7**, 993–1002.

14 Greensmith, H. W. (1964) Rupture of rubber. XI. Tensile rupture and crack growth in a noncrystallizing rubber. *J. Polym. Sci* **8**, 1113–1128.

15 Gent, A. N., Lindley, P. B. and Thomas, A. G. (1964) Cut growth and fatigue of rubbers. I. The relationship between cut growth and fatigue. *J. Appl. Polym. Sci.* **8**, 455–466 (Reprinted in *Rubber Chem. Technol.* **38**, 292–300, 1965).

16 Lake, G. J. and Lindley, P. B. (1964) Cut growth and fatigue of rubbers. II. Experiments on a noncrystallizing rubber. *J. Appl. Polym. Sci.* **8**, 455–466 (Reprinted in *Rubber Chem. Technol.* **38**, 301–313, 1965).

17 Paris, P. C., Gomez, M. P.. and Anderson, W. P. (1961) A rational analytic theory of fatigue. *Trends Eng.* **13**, 9–14.

18 Mars, W. V. and Fatemi, A. (2003) Factors that affect the fatigue life of rubber: A literature survey. *Rubber Chem. Technol.* **76**, (at press).

19 ASTM Standard D4482-99 (2002) *Standard test method for rubber property-extension cycling fatigue*, ASTM, West Conshohocken, PA.

20 Young, D. G. (1990) Application of fatigue methods based on fracture mechanics for tire compound development. *Rubber Chem. Technol.* **63**, 567–581.

21 Young, D. G. (1985) Dynamic property and fatigue propagation research on tire sidewall and model compounds. *Rubber Chem. Technol.* **58**, 785–805.

22 Cadwell, S. M., Merrill, R. A., Sloman, C. M. and Yost, F. L. (1940) Dynamic fatigue life of rubber. *Ind. Eng. Chem.* **12**, 19–23. (Reprinted in *Rubber Chem. Technol.* **13**, 304–315, 1940).

23 Lindley, P. B. (1973) Relation between hysteresis and the dynamic crack growth resistance of natural rubber. *Int. J. Fract.* **9**, 449–461.

24 Mars, W. V. and Fatemi, A. (2003) A phenomenological model for the effect of R ratio on fatigue in strain crystallizing rubber. *Rubber Chem. Technol.* **76**, (at press).

25 Lake, G. J. and Lindley, P. B. (1965) The mechanical fatigue limit for rubber. *J. Appl. Polym. Sci.*, **9**, 1233–1251. (Reprinted in *Rubber Chem. Technol.* **39**, 348–364, 1966).

26 Lake, G. J. (1995) Fatigue and fracture of elastomers. *Rubber Chem. Technol.* **68**, 435–460.

27 Stephens, R. I., Fatemi, A., Stephens, R. R. and Fuchs, H. O. (2000) *Metal Fatigue in Engineering*, 2nd Edn, Wiley-Interscience, NY.